



Measurement of the Dalitz plot slope parameters for $K^- \rightarrow \pi^0 \pi^0 \pi^-$ decay using ISTRAP detector

I.V. Ajinenko, S.A. Akimenko, G.I. Britvich, K.V. Datsko, A.P. Filin, A.V. Inyakin, A.S. Konstantinov, V.F. Konstantinov, I.Y. Korolkov, V.M. Leontiev, V.P. Novikov, V.F. Obraztsov, V.A. Polyakov, V.I. Romanovsky, V.I. Shelikhov, N.E. Smirnov, O.G. Tchikilev, V.A. Uvarov, O.P. Yushchenko

Institute for High Energy Physics, Protvino, Russia

V.N. Bolotov, S.V. Laptev, A.R. Pastsjak, A.Yu. Polyarush, R.Kh. Sirodeev

Institute for Nuclear Research, Moscow, Russia

Received 10 June 2003; accepted 19 June 2003

Editor: L. Montanet

Abstract

The Dalitz plot slope parameters g , h and k for the $K^- \rightarrow \pi^0 \pi^0 \pi^-$ decay have been measured using in-flight decays detected with the ISTRAP setup operating in the 25 GeV negative secondary beam of the U-70 PS. About 252 K events with four-momenta measured for the π^- and four involved photons were used for the analysis. The values obtained $g = 0.627 \pm 0.004(\text{stat}) \pm 0.010(\text{syst})$, $h = 0.046 \pm 0.004(\text{stat}) \pm 0.012(\text{syst})$, $k = 0.001 \pm 0.001(\text{stat}) \pm 0.002(\text{syst})$ are consistent with the world averages dominated by K^+ data, but have significantly smaller errors.

© 2003 Published by Elsevier B.V. Open access under [CC BY license](https://creativecommons.org/licenses/by/4.0/).

1. Introduction

The determination of the Dalitz plot slope parameters for the $K^\pm \rightarrow (3\pi)^\pm$ decays is of interest for the Chiral Perturbation Theory (ChPT) and as a check on the direct CP violation. The latter would manifest itself by the difference between the K^+ and K^- Dalitz plot distributions (see, for example, [1]).

The square of the matrix element of the τ' ($K^\pm \rightarrow \pi^0 \pi^0 \pi^\pm$) decay can be written as

$$|A(K^\pm \rightarrow 3\pi)|^2 \propto 1 + gY + hY^2 + kX^2 + \dots, \quad (1)$$

where $X = (s_1 - s_2)/m_\pi^2$ and $Y = (s_3 - s_0)/m_\pi^2$ are the Dalitz variables, and the parameters g – k are the “Dalitz plot slopes”. Here $s_i = (p_K - p_i)^2$, $s_0 = \frac{1}{3}(s_1 + s_2 + s_3)$, p_K and p_i are the K^\pm and π_i four-momenta (π_3 is the odd pion).

The direct CP violation could be detected by the observation of the following charge asymmetry:

$$(\delta g)_{\tau'} = \frac{g^+ - g^-}{g^+ + g^-}. \quad (2)$$

E-mail address: uvarov@sirius.ihep.su (V.A. Uvarov).

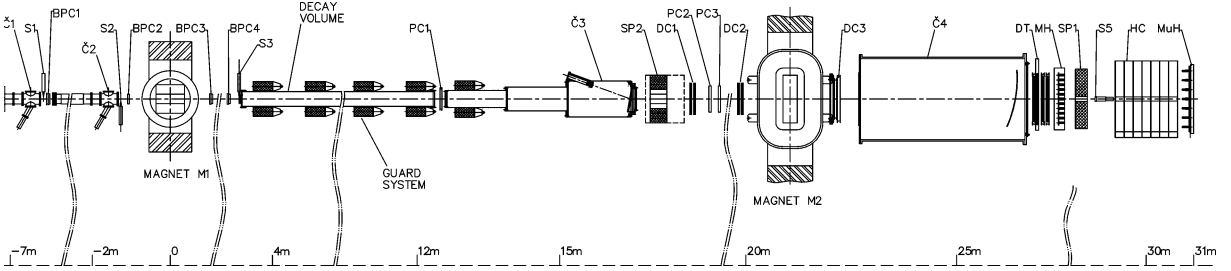


Fig. 1. The side view of the “ISTRA+” detector.

The theoretical predictions for the asymmetry $(\delta g)_{\tau'}$ in the framework of the Standard Model (SM) were originally spread in the wide range of $\sim 2 \times 10^{-6}$ – 10^{-3} [2]. Over last years they have converged to the value of $\sim 10^{-5}$ [1,3]. In a wide class of possible supersymmetric extensions of the SM larger values are possible. For example, in the Weinberg model [4] the value of $\sim 2 \times 10^{-4}$ is predicted [5].

This topic has been attracting significant interest in the recent years. The comparison of the results of the latest K^+ experiment [6] with the only one existing K^- measurement [7] leads to the value of $(\delta g)_{\tau'} = 0.117 \pm 0.022$, i.e., 5.3 sigma effect.

Recently the CP conserving amplitudes for the $K \rightarrow 3\pi$ decays were recalculated in ChPT at the next-to-leading order [8]. In this view a new high statistics measurement for the $K \rightarrow 3\pi$ decays is desirable.

These observations encourage us to perform a new measurement of the Dalitz plot slope parameters g , h and k for the $K^- \rightarrow \pi^0 \pi^0 \pi^-$ decay, based on the statistics of about 250 K events.

2. Experimental setup

The experiment has been performed at the IHEP proton synchrotron U-70 with the experimental apparatus “ISTRA+” which is a modification of the “ISTRA-M” setup [9] and described in some details in our recent papers [10], where studies of the K_{e3}^- and $K_{\mu 3}^-$ decays have been presented. The setup is located in the negative unseparated secondary beam with the following parameters during the measurements: the momentum is ~ 25 GeV/c with $\Delta p/p \sim 2\%$, the admixture of kaons is $\sim 3\%$, and the total intensity is $\sim 3 \times 10^6$ per spill.

The side view of the “ISTRA+” detector is shown in Fig. 1. The momentum and the direction of the beam particle, deflected by the magnet M1, is measured with four proportional chambers BPC1–BPC4. The kaon identification is done by three threshold gas Cherenkov counters Č0–Č2. The momenta of the secondary charged particles, deflected in the vertical plane by the magnet M2, are measured with three proportional chambers PC1–PC3, with three drift chambers DC1–DC3, and with four planes of drift tubes DT. The secondary photons are registered by the lead glass electromagnetic calorimeters SP1 and SP2. To veto low energy photons the decay volume is surrounded by the guard system of eight lead glass rings and by the SP2. The wide aperture threshold helium Cherenkov counters Č3 and Č4 are used to trigger the electrons and are not relevant for the present Letter. In Fig. 1, HC is a scintillator-iron sampling hadron calorimeter, MH is a scintillator hodoscope used to solve the reconstruction ambiguity for multitrack events and improve the time resolution of the tracking system, MuH is a muon hodoscope.

The trigger is provided by the scintillation counters S1–S5, the Cherenkov counters Č0–Č2, and the sum of the amplitudes for the last dinodes of the calorimeter SP1 (see Ref. [10] for details). The latter serves to suppress the $K^- \rightarrow \mu^- \bar{\nu}_\mu$ decay.

3. Event selection

About 363 M and 332 M events were collected during two physics runs in Spring 2001 and Autumn 2001. These experimental data are supported by about 260 M events generated with the Monte Carlo program GEANT3 [11]. The Monte Carlo simulation includes a realistic description of the experimental setup: the decay volume entrance windows, the track chamber

windows, gas, sense wires and cathode structures, the Cherenkov counter mirrors and gas, the showers development in the electromagnetic calorimeters, etc. The details of the reconstruction procedure have been presented in Ref. [10], here only key points relevant to the $K^- \rightarrow \pi^- \pi^0 \pi^0$ event selection are described.

The data processing starts with the beam particle reconstruction in the proportional chambers BPC1–BPC4, and then with the secondary tracks reconstruction in the tracking system PC1–PC3, DC1–DC3 and DT. Finally, the electromagnetic showers are looked for in the calorimeters SP1 and SP2. The method of the photons reconstruction is based on the Monte Carlo generated patterns of showers. To suppress leptonic decays of kaons the particle identification is used [10]. The muons are identified using the information from the calorimeters SP1 and HC. The electrons are identified using the ratio of the energy of the shower, detected in the SP1 and associated with the track of the electron, and the momentum of the electron.

At the first step of the event selection only the measurements of the beam and secondary charged particles are used. Those events are selected which satisfy the following requirements:

- only one beam track and only one negative secondary track are detected;
- the probability of the vertex fit, $CL(\chi^2)$, is more than 0.01;
- the decay vertex is in the region before the calorimeter SP2 ($400 \text{ cm} < z < 1650 \text{ cm}$), and its transverse deviation from the setup axis is less than 10 cm;
- the angle between the beam track and the secondary track is more than 2.5 mrad;
- the transverse momentum of the secondary track with respect to the beam direction is less than $150 \text{ MeV}/c$;
- the secondary track is not identified as an electron or as a muon.

At the second step of the event selection the measurements of the showers in the calorimeters SP1 and SP2 are used. The following requirements are used to choose the photons (showers):

- the distance between the shower in the calorimeter SP1 and the intersection of the secondary track

with the transverse plane of the SP1 is more than 1.5 cm along the magnetic field of the M2 and more than 9 cm in the transverse plane;

- the photon energy is more than 0.7 GeV, but is more than 1.4 GeV when the photon is detected in three or less cells of the calorimeter SP1;
- for events where the secondary track is not associated with any shower in the calorimeter SP1 and with any hit in the hodoscope MH the photon energy is more than 1.4 GeV;
- the energy of the photon found in the multishower cluster is more than 2 GeV.

For each selected $\gamma\gamma$ pair the deviation of its effective mass from the π^0 mass, $\Delta M(\gamma\gamma) = M(\gamma\gamma) - m(\pi^0)$, is calculated. If this deviation is in the range of $|\Delta M(\gamma\gamma)| < 50 \text{ MeV}$, the $\gamma\gamma$ pair is considered as a candidate of the π^0 decay. Then, if this $\gamma\gamma$ pair is taken as a π^0 decay, the four-momenta of its photons are multiplied by a factor $\lambda = m(\pi^0)/M(\gamma\gamma)$. The π^0 detection is illustrated in Fig. 2a, where the spectrum of the effective masses of the “best” $\gamma\gamma$ pairs, i.e., the pairs with the smallest value of $|\Delta M(\gamma\gamma)|$, is shown for the selected events with at least four detected photons. In further selections all combinatorial π^0 candidates are used, not only the “best”.

At the third step of the event selection the sample of the $K^- \rightarrow \pi^- \gamma\gamma\gamma\gamma$ events with two $\pi^0 \rightarrow \gamma\gamma$ decays is collected. For this sample the further selection is done by the requirements that the measured value of the kaon mass is in the range of $|M(\pi^- \pi^0 \pi^0) - m(K^-)| < 80 \text{ MeV}$ (see Fig. 2b) and then the event passes the kinematical 6C-fit for the $K^- \rightarrow \pi^- \pi^0 \pi^0$ hypothesis. The efficiency of the last cut is about 89%. Both requirements are considered for all possible combinations of photons and the best 6C-fit hypothesis is chosen.

Using the mentioned above selection criteria for the $K^- \rightarrow \pi^- \pi^0 \pi^0$ decay we have collected 252 K completely reconstructed events. The corresponding numbers of accepted Monte Carlo events are about ten times larger than in the experiment. The surviving background, which is mainly due to kaon decays to other allowed modes, is estimated from the Monte Carlo simulation to be less than 0.04%.

The detailed event reduction statistics is given in Table 1. The difference in the fraction of the selected events for two runs is due to the higher threshold in

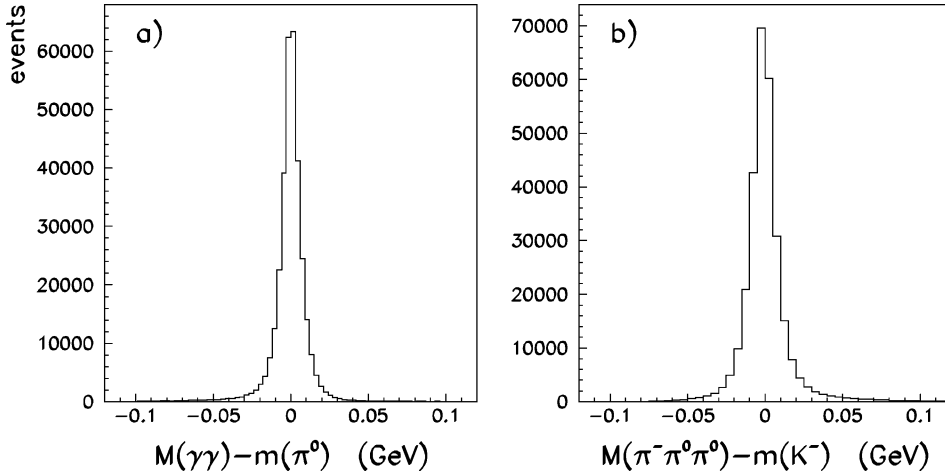


Fig. 2. (a) The deviation $\Delta M(\gamma\gamma) = M(\gamma\gamma) - m(\pi^0)$ of the effective mass of the $\gamma\gamma$ pair with the smallest value of $|\Delta M(\gamma\gamma)|$ in the selected events with at least four detected photons. (b) The deviation $\Delta M(\pi^-\pi^0\pi^0) = M(\pi^-\pi^0\pi^0) - m(K^-)$ of the effective mass of the $\pi^-\pi^0\pi^0$ system with the best photon combination in the selected events.

Table 1
The event reduction statistics for two physics runs

Run	Spring 2001	Autumn 2001
Total number of events	363 M	332 M
Beam track reconstructed	269 M	248 M
Secondary track(s) reconstructed	121 M	124 M
Number of events written on DST	93 M	108 M
K^- and π^- selected (all cuts of the 1st step)	4882 K	7432 K
At least four γ selected (all cuts of the 2nd step)	83 K	244 K
Two π^0 selected	69 K	218 K
$K^- \rightarrow \pi^-\pi^0\pi^0$ selected (all cuts of the 3rd step)	59 K	193 K

the SPI at the trigger level for the second run, i.e., the initial statistics of the first run contains more $K^- \rightarrow \mu^- \bar{\nu}_\mu$ decays than the initial statistics of the second run.

4. Analysis

To determine the parameters g , h and k in Eq. (1) the uncorrected distribution $\rho(X, Y)$ of the event density on the Dalitz plot was analysed. This distribution is shown in Fig. 3 for the selected $K^- \rightarrow \pi^-\pi^0\pi^0$ events. At first the background contamination was subtracted from the Dalitz plot. The contamination was estimated from the Monte Carlo simulation of the particle interaction with the material of the detector and of the kaon decay including all decay modes with the branching ratios more than 1%. The corresponding

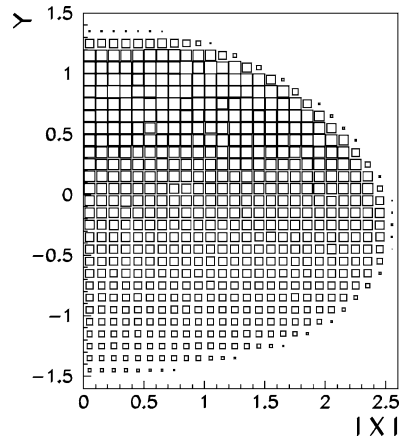


Fig. 3. The Dalitz plot, $Y = (s_3 - s_0)/m_\pi^2$ vs. $X = (s_1 - s_2)/m_\pi^2$, for the selected $K^- \rightarrow \pi^-\pi^0\pi^0$ events (uncorrected).

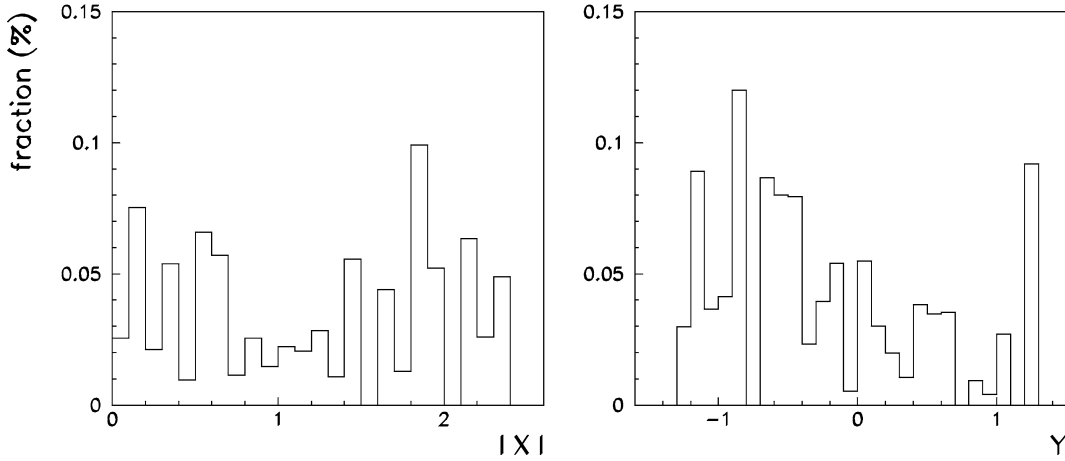


Fig. 4. The fraction of the background contamination as a function of the Dalitz plot variable estimated from Monte Carlo simulation.

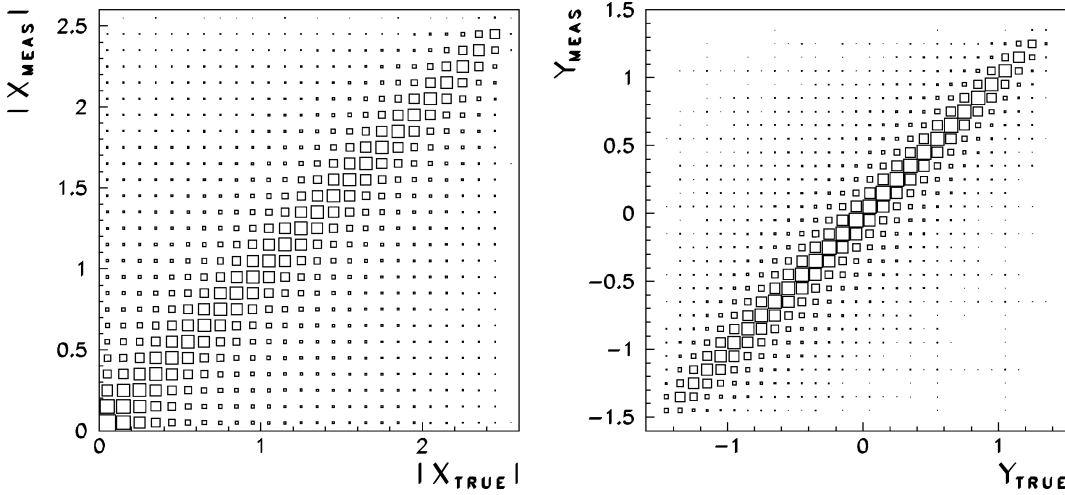


Fig. 5. The “measured” values of the Dalitz plot variables $|X|$ and Y vs. the “true” ones estimated from Monte Carlo simulation.

branching ratios and matrix elements in this simulation were taken from the PDG [12]. In Fig. 4 the fraction of the background contamination is shown as a function of the Dalitz plot variables $|X|$ and Y .

The background subtracted distribution $\rho'(X, Y)$ was fitted by the method of least squares with the function:

$$\rho'(X, Y) \propto F_1(X, Y) + gF_2(X, Y) + hF_3(X, Y) + kF_4(X, Y), \quad (3)$$

where $F_k(X, Y)$ are the distributions for the w_k -weighted Monte Carlo $K^- \rightarrow \pi^- \pi^0 \pi^0$ events gen-

erated with the constant matrix element and reconstructed with the same program as for the real events. The weight factors $w_1 = 1$, $w_2 = Y_{\text{true}}$, $w_3 = Y_{\text{true}}^2$ and $w_4 = X_{\text{true}}^2$ are given by the “true” values of X and Y , but the bins of $F_k(X, Y)$ are given by the “measured” ones. This method allows to avoid the systematic errors [13] due to the “migration” of the events on the Dalitz plot because of the finite experimental resolution. Fig. 5 illustrates the Monte Carlo estimated experimental resolution for the variables $|X|$ and Y , where the “measured” values are shown versus the “true” ones.

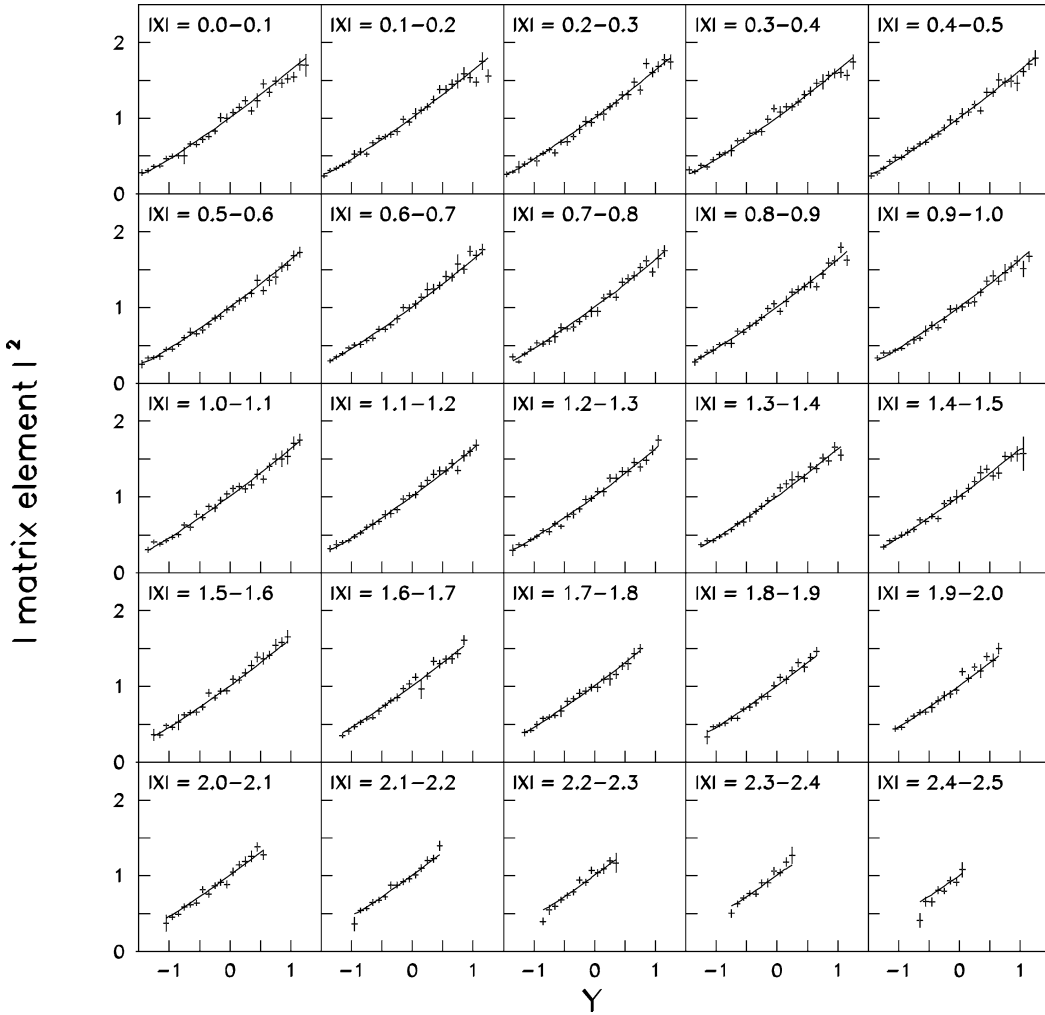


Fig. 6. The matrix element dependence on the variable Y in the different intervals of the variable $|X|$ for the $K^- \rightarrow \pi^- \pi^0 \pi^0$ decay. The curves are the result of the fit to the function (3).

5. Results

The result of the least squares fit is illustrated in Fig. 6, where the matrix element

$$|A(K^- \rightarrow \pi^- \pi^0 \pi^0)|^2 = C \frac{\rho'(X, Y)}{F_1(X, Y)} \quad (4)$$

for the $K^- \rightarrow \pi^- \pi^0 \pi^0$ decay is shown as a function of Y in the different intervals of $|X|$. The normalization constant C in Eq. (4) provides the value of $|A|^2 = 1$ at the point $(X = 0, Y = 0)$. The integrated dependences of the matrix element on the variables Y and $|X|$ are shown in Fig. 7.

The values of the Dalitz plot slope parameters are found to be

$$g = 0.627 \pm 0.004 \pm 0.010,$$

$$h = 0.046 \pm 0.004 \pm 0.012,$$

$$k = 0.001 \pm 0.001 \pm 0.002$$

with $\chi^2/\text{ndf} = 502/558$. Here the first errors are statistical and the second ones are systematic.

In the determination of the systematic errors of the slope parameters measurement the following contributions were taken into account.

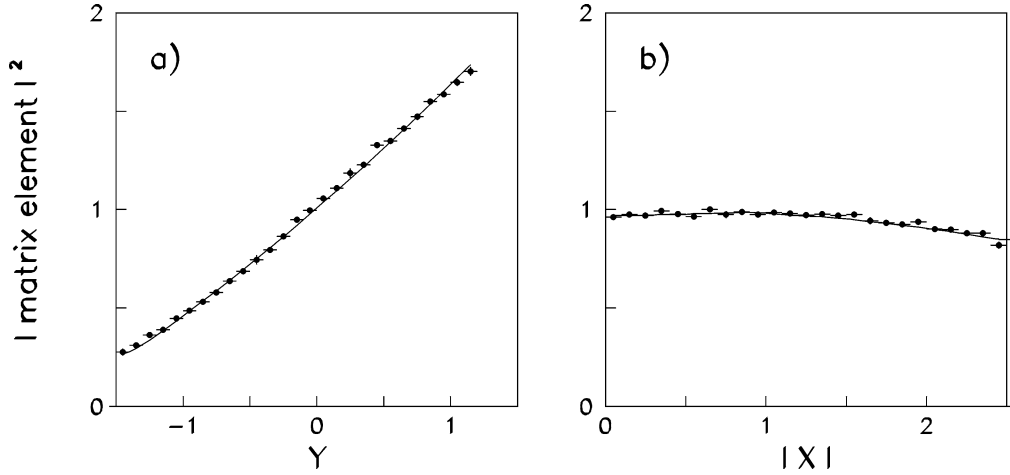


Fig. 7. The integrated dependences of the matrix element on the variables (a) Y and (b) $|X|$ for the $K^- \rightarrow \pi^- \pi^0 \pi^0$ decay. The curves are the result of the fit to the function (3).

- Two samples of the events collected in the runs (Spring and Autumn 2001) with some differences in characteristics of the setup were analysed separately (the corresponding contributions to the systematic errors are $\Delta g = 0.001$, $\Delta h = 0.001$ and $\Delta k = 0.0002$).
- To avoid some uncertainties at the edge of the Dalitz plot the extreme bins of this plot were cut ($\Delta g = 0.001$, $\Delta h = 0.002$, $\Delta k = 0.0004$).
- The energy threshold of the selected photons was increased from the value of 0.7 GeV to 2 GeV ($\Delta g = 0.006$, $\Delta h = 0.007$, $\Delta k = 0.001$).
- The mass and energy ranges used in the event selection criteria were varied from the value of 30 MeV to 80 MeV with and without introducing a factor $\lambda = m(\pi^0)/M(\gamma\gamma)$ ($\Delta g = 0.003$, $\Delta h = 0.004$, $\Delta k = 0.001$).
- The background contamination estimated from the Monte Carlo simulation was not subtracted from the Dalitz plot before the least squares fit ($\Delta g = 0.001$, $\Delta h = 0.001$, $\Delta k = 0.0002$).
- The particle identification of the secondary track was not used ($\Delta g = 0.001$, $\Delta h = 0.001$, $\Delta k = 0.0003$).
- The electromagnetic showers in the calorimeter SP2 were not used in the photon reconstruction ($\Delta g = 0.006$, $\Delta h = 0.007$, $\Delta k = 0.0014$).
- The upper edge of the decay vertex position was varied along the setup axis between the chamber

PC1 and the calorimeter SP2 ($\Delta g = 0.004$, $\Delta h = 0.005$, $\Delta k = 0.001$).

- The cut applied to the angle between the beam and secondary tracks was varied from 1.5 to 3.5 mrad ($\Delta g = 0.001$, $\Delta h = 0.001$, $\Delta k = 0.0003$).

6. Summary and conclusion

The Dalitz plot slope parameters for the $K^- \rightarrow \pi^- \pi^0 \pi^0$ decay have been measured using the “ISTRA+” spectrometer. It is an update of our preliminary presentation [14]. The results of our measurement, the world averages [12] and the results of previous experiments [6,7,15–21] on the $K^\pm \rightarrow \pi^\pm \pi^0 \pi^0$ decays are presented in Fig. 8. Among the previous experiments there are eight measurements of the K^+ decay, but only one of the K^- decay. Our values of the slope parameters g and h are consistent with the world averages dominated by K^+ measurements. The difference between the values of the linear slope g obtained for the $K^- \rightarrow \pi^- \pi^0 \pi^0$ decay in our experiment and in another one [7] is 1.9 standard deviations.

Using the same rules as in the PDG [12] (without the data [20,21] obtained from the linear fit only) and adding our measurement, one can obtain the world average values of the linear slope g for the K^+ and K^- decays separately: $g^+ = 0.684 \pm 0.033$ and $g^- = 0.617 \pm 0.018$. They give for the charge asymmetry (2) the value of $(\delta g)_{\tau'} = 0.051 \pm 0.028$.

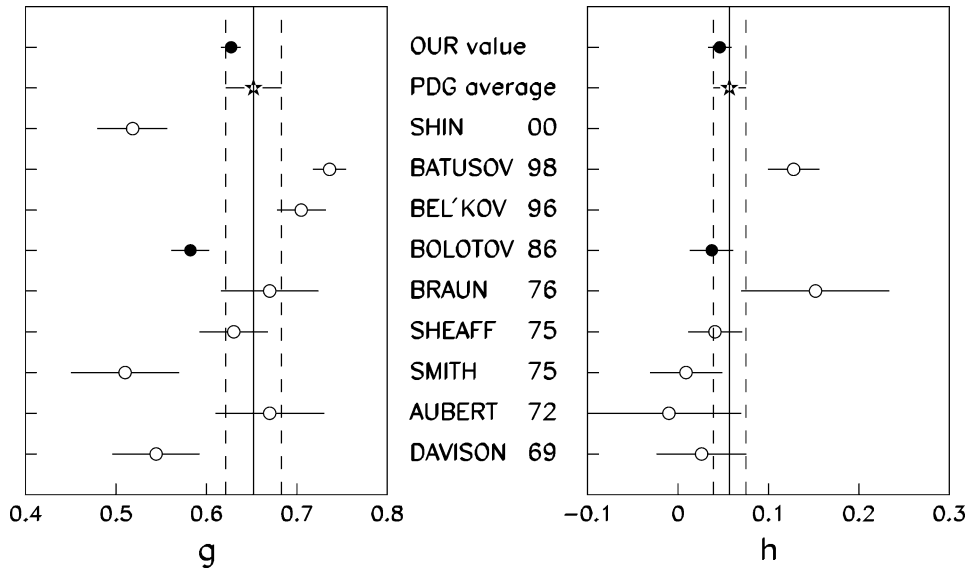


Fig. 8. The Dalitz plot slope parameters g and h for the $K^- \rightarrow \pi^- \pi^0 \pi^0$ (solid circles), $K^+ \rightarrow \pi^+ \pi^0 \pi^0$ (open circles) and $K^\pm \rightarrow \pi^\pm \pi^0 \pi^0$ (solid stars) decays.

The analytical expressions of the CP conserving $K \rightarrow 3\pi$ amplitudes with single parameter functions, recalculated in the framework of ChPT at the next-to-leading order, were fitted in Ref. [8] to all available $K \rightarrow 2\pi$ and $K \rightarrow 3\pi$ data. The result of this global fit gives the following predictions for physical observables of the $K^\pm \rightarrow \pi^\pm \pi^0 \pi^0$ decays: $g = 0.638$, $h = 0.074$ and $k = 0.0045$. These predictions agree within 1–2 standard deviations with our results.

Acknowledgements

The work is supported by the RFBR contract No. 03-02-16330.

References

- [1] G. D'Ambrosio, G. Isidori, *Int. J. Mod. Phys. A* 13 (1998) 1.
- [2] L. Maiani, N. Paver, in: L. Maiani, et al. (Eds.), *The 2nd DAΦNE Physics Handbook*, Vol. 1, INFN–LNF, Frascati, 1995, p. 51;
- [3] G. D'Ambrosio, G. Isidori, G. Martinelli, *Phys. Lett. B* 480 (2000) 164.
- [4] S. Weinberg, *Phys. Rev. Lett.* 37 (1976) 657.
- [5] E. Shabalin, Preprint ITEP 8-98, 1998.
- [6] V.Y. Batusov, et al., *Nucl. Phys. B* 516 (1998) 3.
- [7] V.N. Bolotov, et al., *Sov. J. Nucl. Phys.* 44 (1986) 73.
- [8] J. Bijnens, P. Dhonte, F. Persson, *Nucl. Phys. B* 648 (2003) 317.
- [9] V.N. Bolotov et al., Preprint IHEP 95-111, Protvino, 1995.
- [10] I.V. Ajinenko, et al., *Phys. At. Nucl.* 65 (2002) 2064; I.V. Ajinenko, et al., *Phys. At. Nucl.* 66 (2003) 105.
- [11] R. Brun et al., Preprint CERN-DD/EE/84-1.
- [12] Particle Data Group, K. Hagiwara, et al., *Phys. Rev. D* 66 (2002) 010001.
- [13] V.B. Anikeev, V.P. Zhigunov, *Phys. Part. Nucl.* 24 (1993) 989.
- [14] I.V. Ajinenko et al., Preprint IHEP 2002-16, Protvino, 2002.
- [15] D. Davison, et al., *Phys. Rev.* 180 (1969) 1333.
- [16] B. Aubert, et al., *Nuovo Cimento* 12A (1972) 509.
- [17] K.M. Smith, et al., *Nucl. Phys. B* 91 (1975) 45.
- [18] M. Sheaff, *Phys. Rev. D* 12 (1975) 2570.
- [19] H. Braun, et al., *Lett. Nuovo Cimento* 17 (1976) 521.
- [20] A. Bel'kov, et al., in: Z. Ajduk, A.K. Wroblewski (Eds.), *Proc. of the 28th Int. Conf. on High Energy Physics, Warsaw, 1996*, Vol. 2, World Scientific, Singapore, 1997, p. 1204.
- [21] Y.-H. Shin, et al., *Eur. Phys. J. C* 12 (2000) 627.
- [22] A.A. Bel'kov, et al., *Phys. Lett. B* 232 (1989) 118.